Parameter Estimation of Photovoltaic Module under Dynamic Weather Using an Enhanced Grey Wolf Optimizer

Kai He, Yong Zhang*

Abstract—In view of the problem of low parameter estimation accuracy in triple diode photovoltaic (PV) modules under dynamic weather conditions, a novel enhanced grey wolf optimizer (FCGWO) is proposed. It incorporates the fitness-distance balance (FDB) selection method into the chaos learning strategy to improve convergence performance and population diversity. Firstly, based on the ergodicity and randomness of the improved Tent chaotic map, search range of the algorithm is expanded to explore more potential areas. Secondly, the chaos learning employs the guiding approach to make the average position of population gradually approach optimal solution, thereby enhancing the global exploitation performance. Thirdly, the FDB selection method considers both the fitness and distance of solutions, strikes a balance between global exploration and local exploitation, and increases the probability of escaping from local optima. Then, FCGWO is compared and evaluated with eight other algorithms on CEC2022 test suite. Finally, FCGWO is employed to estimate the parameters of an actual PV module (Shell ST40) modeled by triple diode under dynamic weather state. Experimental results demonstrate that FCGWO attains the best estimation accuracy under different irradiance and temperature conditions, indicating its great potential for application in PV modules.

Index Terms—Photovoltaic module, parameter estimation, chaos learning strategy, fitness-distance balance, grey wolf optimizer

I. INTRODUCTION

IN the context of today's growing energy demand and increasingly urgent environmental protection, photovoltaic (PV) power generation has become the focus of the global energy field with its clean and renewable advantages [1, 2]. Whereas, the stable operation, performance evaluation and optimization of PV systems cannot be achieved without accurate parameter estimation of PV models [3]. As time progresses, the natural environment is constantly changing. Weather factors such as fluctuations in irradiance intensity and temperature make the operating state of the PV system extremely complicated [4]. Consequently, researching the estimation of PV model parameters under dynamic weather conditions holds substantial practical significance [5].

Currently, the methods for estimating PV model parameters can be classified into analytical methods [6], numerical optimization methods, and meta-heuristic algorithms [7]. Analytical methods solve the PV model parameters by constructing the explicit equations of the PV model based on a few physical data provided by PV module manufacturers or obtained through actual measurement. This method features low computational complexity and simplicity, yet it has low accuracy and is susceptible to key data and noise [8]. Numerical optimization methods, on the other hand, accurately extract model parameters by minimizing the root mean square error (RMSE) between the simulated and measured I-V curves. Common methods include the Newton-Raphson method, pattern search method, etc. These types of methods are sensitive to initial values and have poor reliability [9]. Meta - heuristic algorithms, on the other hand, possess several notable advantages. They are characterized by straightforward calculations, show little sensitivity to initial values, and can achieve high optimization precision.

In recent years, a plethora of novel meta-heuristic algorithms have emerged, such as multi-strategy whale optimization algorithm (MSWOA) [10], dual-population firefly algorithm based on gender differences (DFAGD) [11], improved seagull optimization algorithm with elite reserve (ISOAE) [12], white shark optimizer (WSO) [13], improved particle swarm optimization algorithm (SCOPSO) [14]. Among them, numerous meta-heuristic algorithms have found applications in the PV models parameter estimation, such as coyote optimization algorithm (COA), which was used to estimate 9 unknown parameters of KC200GT and MSX-60 modules established by triple diode model (TDM) [15]. In [16], Harris hawks optimization (HHO) was utilized to extract the parameters of multi-crystal KC200GT and monocrystalline CS6K280M built by TDM. Da Wang et al. [17] put forward a novel heterogeneous differential evolution algorithm (HDE), which enhanced the exploration and exploitation process of HDE by introducing two novel variation strategies and an information exchange mechanism, experimental results confirm the effectiveness of HDE. Mahmoud A. Soliman et al. [18] designed equilibrium optimizer algorithm (EOA) to identify the parameters of a TDM PV module model. In [19], marine predators algorithm (MPA) is employed to extract the electrical parameters of PV module models of KC200GT and Solarex MSX-60 PV panels established by TDM. Kunjie Yu et al. [20] presented an improved JAYA optimization algorithm (IJAYA) by adding adaptive weights and experience-based learning strategies to enhance the performance. IJAYA has been applied to deal with the parameter identification problem of single diode model (SDM), double diode model (DDM) of PV cells and PV module. Mohamed Abdel-Basset et al. [21] introduced the rank-based generalized normal distribution optimization (RGNDO) algorithm. This algorithm uses a precocity convergence approach and

Kai He is a doctoral candidate of School of Electronic and Information Engineering, University of Science and Technology Liaoning, Anshan, Liaoning 114051, China (e-mail: kaihe@ustl.edu.cn).

Yong Zhang is a professor of School of Electronic and Information Engineering, University of Science and Technology Liaoning, Anshan, Liaoning 114051, China (* Corresponding author, phone: 8615841209991; e-mail: zy9091@163.com).

a sort-based update method to speed up convergence, and its effectiveness is verified on the STP 6-120/36, KC200GT, RTC cell, and Ultra 85-P built with TDM. Mohamed Abd Elaziz et al. [22] introduce an improved opposition-based whale optimization algorithm (OBWOA), which uses reverse learning strategy to broad the search space of WOA. It has been demonstrated in SDM, DDM and TDM of PV cells. An improved teaching-learning-based optimization (ITLBO) algorithm was used to extract the parameters of SDM, DDM and TDM of PV modules [23]. In the teacher stage, teachers choose distinct teaching strategies according to the learners' specific levels. During the learner stage, a novel learning strategy was put forward to strike a balance between exploration and exploitation. Experimental results indicated that ITLBO outperformed the comparative algorithms in terms of accuracy. Lemin Peng et al. [24] proposed an information sharing search boosted whale optimizer with Nelder-Mead simplex (ISNMWOA). WOA can conduct a global search for PV model parameters. The information sharing search strategy conducts a rough local search on the generated feasible solutions. Moreover, the Nelder-Mead simplex can conduct a more refined local search near the optimal parameters. The results demonstrate that ISNMWOA outperforms the comparison algorithms in terms of results obtained from SDM, DDM, TDM of PV cells and PV module models. An enhanced adaptive butterfly optimization algorithm (EABOA) was used to identify parameters of PV models [25]. The algorithm proposes a position search equation and a good-point set to balance exploration and exploitation, and identify unknown parameters of SDM, DDM and PV module models. When compared with other algorithms, the results show that EABOA has higher accuracy.

The above literature shows that many algorithms have made substantial contributions to the estimation of PV parameters. However, it is difficult to estimate the parameters of PV module models constructed using TDM under dynamic weather conditions, and there are few relevant literatures. In recent years, the grey wolf optimizer (GWO) has attracted considerable attention due to its effectiveness in addressing a wide range of optimization problems. For instance, Sharma et al. [26] employed GWO in the automatic generation control of a multi-area ST–thermal power system, demonstrating the algorithm's capability in optimizing classical controllers. Jayabarathi et al. [27] a hybrid GWO for economic dispatch, emphasizing the algorithm's potential in tackling complex optimization scenarios. Gupta et al. [28] introduced a novel random walk GWO, expanding the algorithm's capabilities in random search processes. Evidently, GWO has been proven to be a flexible and efficient optimization approach with successful applications across multiple domains. Notably, however, there have been few reports on its application in PV model estimation. This complex problem and the practical method of GWO are worthy of further discussion and combination. Therefore, this paper proposes an enhanced grey wolf optimizer (FCGWO).

The main contributions of this paper are as follows.

(1) An enhanced grey wolf optimizer is proposed and applied to the parameter estimation of a TDM PV module under dynamic weather conditions.

(2) We integrate the fitness-distance balance selection method into the chaos learning strategy and apply it to the population position update of GWO, which improves the convergence performance and population diversity of GWO.

(3) The performance of FCGWO is assessed by using CEC2022 benchmark set and compared with 8 well - established algorithms. The outstanding performance of FCGWO is confirmed by non-parametric test and statistical analysis.

(4) FCGWO is utilized to estimate the parameters of an actual PV module (Shell ST40) established by TDM under dynamic weather conditions.

The subsequent parts of this paper are arranged as follows.
- Section II details the problem description of PV model.
- Section III describes the proposed FCGWO.
- Section IV shows the evaluation of FCGWO based on CEC2022.
- Section V demonstrates the parameters estimation results of PV modules established by TDM under dynamic weather.
- Section VI discusses the conclusions and future work.

II. PROBLEM DESCRIPTION OF PV MODULE MODEL

A. PV module model

PV modules are assembled through the series and parallel connection of PV cells [29]. Typically, PV cells have SDM, DDM, and TDM. Compared to SDM and DDM, TDM can more comprehensively characterize all the losses in 3 regions of a PV cell [30]. There, we choose TDM to build PV module model, and its equivalent circuit diagram is shown in Fig. 1. The output current I_o of the circuit is calculated as Eq.(1).

$$
\begin{aligned}
I_o = {} & N_p * I_{ph} - \frac{V_o/N_s + R_s * I_o/N_p}{R_p/N_p} \\
& - N_p * I_{sd1} * \left[exp(\frac{q * (V_o/N_s + R_s \cdot I_o/N_p)}{n_1 * k_B * T_K}) - 1 \right] \\
& - N_p * I_{sd2} * \left[exp(\frac{q * (V_o/N_s + R_s \cdot I_o/N_p)}{n_2 * k_B * T_K}) - 1 \right] \\
& - N_p * I_{sd3} * \left[exp(\frac{q * (V_o/N_s + R_s \cdot I_o/N_p)}{n_3 * k_B * T_K}) - 1 \right]
\end{aligned} \tag{1}
$$

Among them, N_p and N_s denote the quantities of PV cells connected in parallel and in series, respectively. I_{ph} is the photogenerated current, I_{sd1}, I_{sd2} and I_{sd3} signify the reverse saturation current of the three diodes, respectively. Moreover, n_1, n_2 and n_3 are the ideal factors corresponding to the three diodes respectively. q stands for the electronic charge, with a value of $1.60217646*10^{-19}$C. k_B refers to Boltzmann's constant, which is $1.3806503*10^{-23}$J/K. V_o is the output voltage of the circuit, T_K represents the cell temperature in Kelvin unit. Additionally, R_s and R_p represent the series and parallel resistance, respectively.

B. Objective function

RMSE is often used as the objective function for estimating the parameters of PV cell and module models [31]. Similarly, this paper also employs (RMSE) to represent the total difference between the actually measured and estimated values, which is expressed as follows.

$$
RMSE = \sqrt{\frac{1}{M} \sum_{i=1}^{M} (I_{o,act}^i - I_{o,est}^i(x))^2} \tag{2}
$$

Where M is the number of measured data, $I_{o,act}$ is supplied by manufacturers or actually measured. According to Eq.(1), there are 9 unknown parameters of the
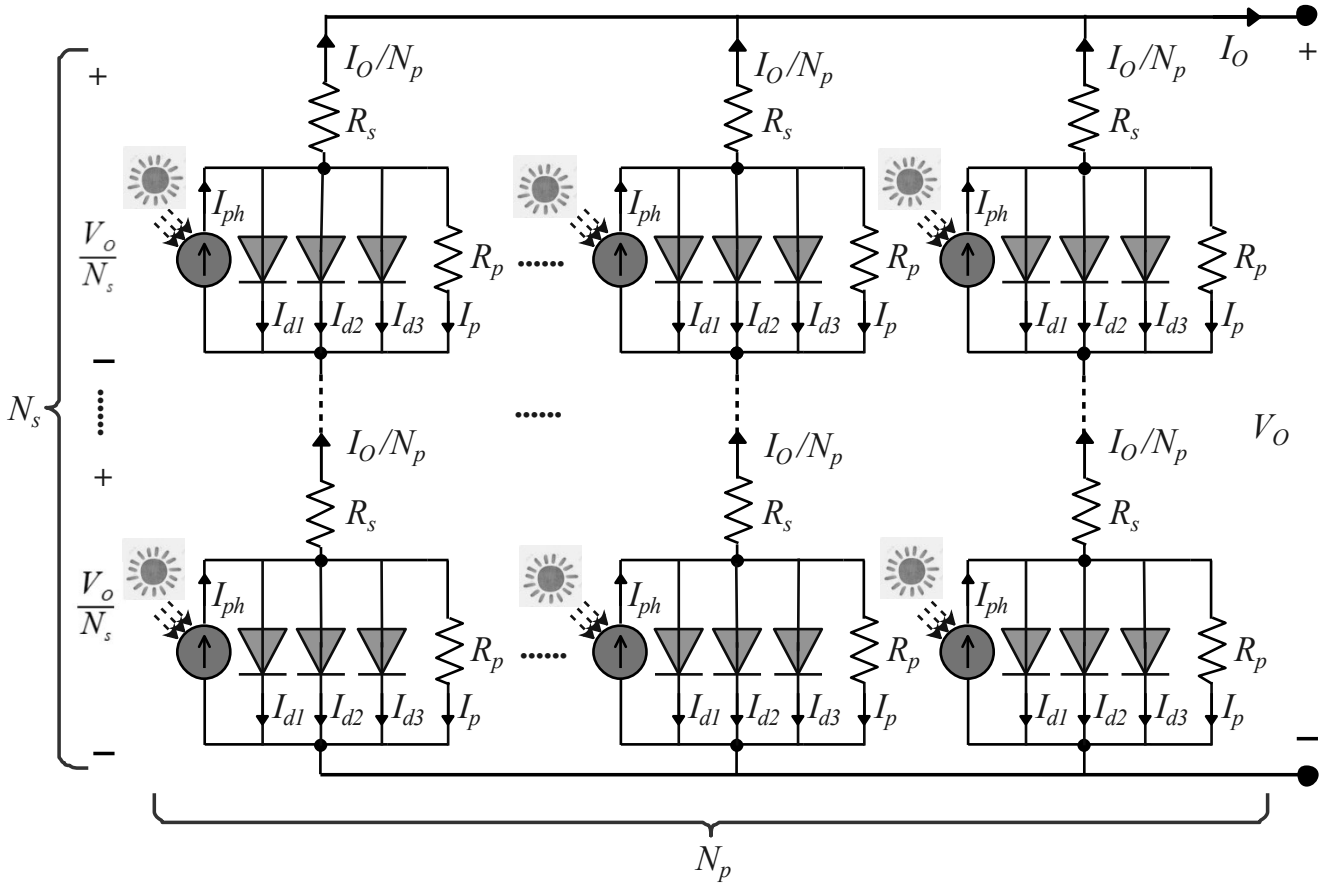
Fig. 1: PV module model by TDM.

PV module model established by TDM, which are $x = I_{ph}, I_{sd1}, I_{sd2}, I_{sd3}, R_s, R_p, n_1, n_2, n_3$. $I_{o,est}(x)$ will be estimated by FCGWO to achieve the minimum RMSE value.

III. THE PROPOSED FCGWO

In this part, we commence by presenting grey wolf optimizer (GWO). Subsequently, we incorporate the fitness-distance balance (FDB) selection method into the chaos learning strategy. This integrated approach is then applied to the position update process of GWO, aiming to enhance both its convergence performance and population diversity.

A. Grey wolf optimizer

Grey wolf optimizer (GWO) is a meta-heuristic optimization algorithm inspired by the social hierarchy and hunting behavior of grey wolf populations in the natural world [32]. In this algorithm, wolves are divided into four levels, α wolf serves as the pack leader and corresponds to the best solution obtained so far; β wolf is the second best solution; δ wolf is the third best solution; ω wolf stands for other solutions.

Initializing: N wolves are randomly distributed in the boundary $[lb, ub]$, and this process is formulated as Eq.(3).

$$X_{i,j} = rand * (ub_j - lb_j) + lb_j, i \in [1, N], j \in [1, D] \quad (3)$$

Where D is the dimension, $X_{i,j}$ is the j-th dimension of the i-th wolf. During the t-th iteration, the position of the i-th wolf is denoted as $X_i^t = \{x_{i,1}, x_{i,2}, \cdots, x_{i,D}\}$. For PV model parameter estimation, the fitness value (RMSE) is calculated by Eq.(2).

Encircling: Based on their fitness values, these grey wolves compete and cooperate with other individuals to find the optimal solution. The mathematical model of how wolves surround their prey is as follows.

$$X^{t+1} = X_p^t - A * |C * X_p^t - X^t| \quad (4)$$

Where X^{t+1} denotes the wolf's position at the next iteration, X_p^t represents the position of the prey during the t-th iteration. Additionally, A and C are coefficient vectors, and their calculation methods are follows.

$$A = a * (2 * r_1 - 1) \quad (5)$$

$$C = 2 * r_2 \quad (6)$$

Where, r_1 and r_2 are random vectors that lie within the interval [0,1] and obey uniform distribution.

$$a = 2 * (1 - t/T) \quad (7)$$

Here, t denotes the current iteration number, while T represents the maximum number of iterations.

Hunting: The position of the i-th grey wolf at the $(t+1)$-th iteration is calculated as follows.

$$X_{i-GWO}^{t+1} = (X_{i1}^t + X_{i2}^t + X_{i3}^t)/3 \quad (8)$$

Among them, X_{i1}^t, X_{i2}^t and X_{i3}^t is calculated as follows.

$$\begin{aligned} X_{i1}^t &= X_\alpha^t - A_1 * |C_1 * X_\alpha^t - X_i^t| \\ X_{i2}^t &= X_\beta^t - A_2 * |C_2 * X_\beta^t - X_i^t| \\ X_{i3}^t &= X_\delta^t - A_3 * |C_3 * X_\delta^t - X_i^t| \end{aligned} \quad (9)$$

Here, X_α^t, X_β^t, and X_δ^t respectively represent the positions of the α wolf, β wolf, and δ wolf during the t-th iteration.

B. FDB-based selection method

During the algorithm's search process, choosing suitable candidate solutions from the population directly impacts the search direction and success [33]. This demands that the candidate solutions contribute maximally to the search. The FDB-based selection method doesn't merely emphasize the fitness value of a solution but also considers the distance factor between solutions [34]. This method stably and effectively identifies one or more candidate solutions that contribute most to the group search process, playing a crucial balancing and guiding role in the algorithm. The FDB score of an individual is defined as follows.

$$\stackrel{m}{\underset{i=1}{}} \forall X_i, S_{X_i} = w * normF_i + (1-w) * normD_i \quad (10)$$

Here, the F-matrix is the fitness value matrix for individuals. The D-matrix represents the distance between each individual within the population and the optimal solution $gbest$. They are normalized to prevent them from dominating each other, denoted as $normF$ and $normD$. w is a weighting coefficient and is taken as 0.5.

C. Chaos learning strategy with FDB-based selection

Although GWO is straightforward and can be applied to various scenarios, it has several drawbacks. These include a lack of sufficient population diversity, an imbalance between exploitation and exploration, and a tendency to converge prematurely. Additionally, GWO's search mode is more focused on exploitation, making it likely to be trapped in local optima [35]. Therefore, GWO requires a new optimization and position mutation strategy. Xueyan Ru [36] creatively proposed a chaotic learning strategy and integrated it into the butterfly optimization algorithm, and the estimation results of parameters for six types of PV cells and six types of module models have confirmed the beneficial effects of this strategy. To further enhance the performance of this strategy, we incorporated the FDB selection method into it, named it chaos learning strategy with FDB-based, abbreviated as FC for short, and applied it to the population position update of GWO to enhance the convergence performance and population diversity. This process is shown in the dotted box in Fig. 2, and is specifically described below.

(a) Chaos phase. Chaos is a prevalent nonlinear phenomenon that uses mapping relationships to generate chaotic sequences between [0,1] and then incorporates these sequences into the solution space of the problem under consideration. This action induces perturbations to the positions of the individuals [37]. The improved Tent chaotic mapping has more extensive randomness and ergodicity, and it is calculated by Eq.(11).

$$z_i = sgn(0.5 - rand) * [(2 * rand) mod 1 + rand/(N * D)] \quad (11)$$

Where sgn is the symbolic function used to regulate the direction of the perturbation, and it supplies the Tent mapping values within the range of [-1,1].

(b) Learning phase. In a population, $gbest$ is supposed to raise the average value of the population to a certain degree, depending on the population's capabilities. The mean position of the population is expressed by Eq.(12).

$$X_m = (\frac{1}{N} \sum_{i=1}^{N} X_{i,1}, \frac{1}{N} \sum_{i=1}^{N} X_{i,2}, \cdots \frac{1}{N} \sum_{i=1}^{N} X_{i,Dim}) \quad (12)$$

In the original chaos learning phase, only the $gbest$ is used for guidance. However, when the $gbest$ falls into the trap of local optima, it will cause the other solutions within the population to gradually approach the $gbest$. Whether it is the subsequent exploration or exploitation, the grey wolf individuals will lose their vitality. Eventually, this will cause the algorithm to converge to a local optimum. Therefore, we utilize the FDB method to select candidate solutions that make substantial contributions to the search as guidance to lead the population. We define the process of the population learning from the average position with respect to this guidance as the learning step, which is presented in Eq.(13).

$$X_{learning} = \begin{cases} z_i * (gbest - X_m) & \text{if } rand < 0.5 \\ z_i * (X_{fdb} - X_m) & \text{otherwise} \end{cases} \quad (13)$$

Where, X_{fdb} is the highest-scoring individual in the population calculated from Eq.(10).

Finally, the wolf individuals update their positions using the learning step, which is expressed as Eq.(14).

$$X_{i-CL}^{t+1} = X_i^t + rand(1, Dim). * X_{learning} \quad (14)$$

To sum up, the chaos learning strategy utilizes the ergodicity and randomness of the Tent chaotic mapping to increase population diversity of GWO. It enables the algorithm to quickly traverse to the promising search regions in the initial stage, reducing invalid searches, thereby accelerating the convergence speed and precision. The introduced FDB-based selection method considers the influences of the fitness and distance of solutions to improve the algorithm's capacity to break free from local optima and strikes a balance between global exploration and local exploitation.

D. Structure of FCGWO

The pseudo-code and flowchart can visually demonstrate the structure, as shown in Algorithm 1 and Fig. 2, separately.

Algorithm 1: The pseudo-code of FCGWO

Input: Initialize parameters.
Output: Optimal solution $gbest$.
1 Randomly initialize population using Eq.(3);
2 Evaluate fitnesses of X, get $gbest$, and update FEs;
3 $T = \lceil maxFEs/N \rceil$, $t = 0$;
4 **while** $FEs <= maxFEs$ && $t <= T$ **do**
5     $t = t + 1$;
6   Define X_α, X_β, and X_δ;
7   **for** $i = 1$ **to** N **do**
8   Calculate X_{i1}, X_{i2} and X_{i3} by Eq.(9);
9   Calculate X_{i-GWO} by Eq.(8);
10   Check boundaries and evaluate X_{i-GWO};
11   Update X_i, $gbest$, and FEs;
12   **end**
13   **for** $i = 1$ **to** N **do**
14   Compute $X_{learning}$ by Eq.(13);
15   Compute X_{i-CL} by Eq.(14);
16   Check boundaries and evaluate X_{i-CL};
17   Update X_i, $gbest$, and FEs;
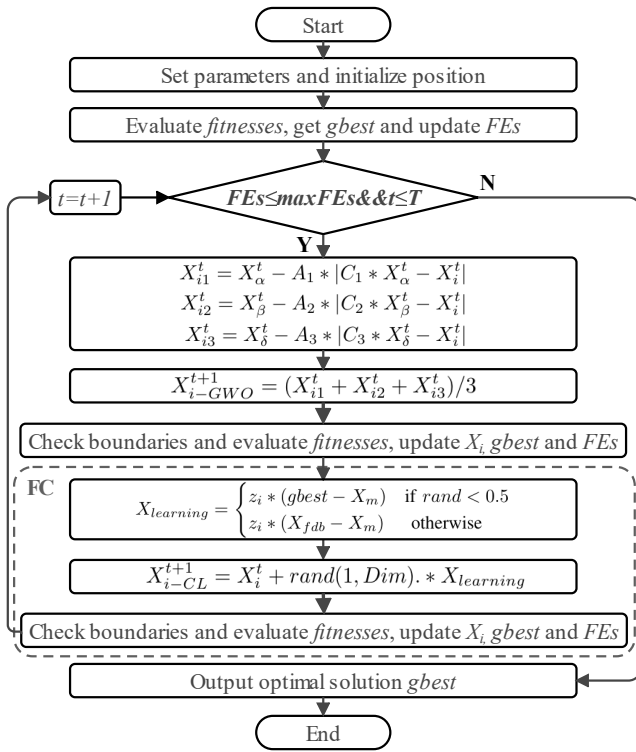18   **end**
19 **end**

Fig. 2: Flowchart of FCGWO.

IV. EVALUATION ON CEC2022

In this section, CEC2022 benchmark test set [38] is employed to validate the performance of FCGWO.

A. Benchmark functions and algorithms parameter setting

CEC2022 benchmark functions have become a widely used test suite. There exist four distinct categories of functions, which are presented in Table I. They are complex to solve and extremely challenging, and can well evaluate the comprehensive performance of algorithms.

TABLE I
CEC2022 BENCHMARK FUNCTIONS INFORMATION.

Type	No.	f_{best}	Function name
Unimodal	f_1	300	Shifted and full Rotated Zakharov
Basic	f_2	400	Shifted and full Rotated Rosenbrock's
	f_3	600	Shifted and full Rotated Expanded Schaffer's f_6
	f_4	800	Shifted and full Rotated Non-Continuous Rastrigin's
	f_5	900	Shifted and full Rotated Lévy
Hybrid	f_6	1800	Hybrid 1 (N=3)
	f_7	2000	Hybrid Function 2 (N=6)
	f_8	2200	Hybrid Function 3 (N=5)
Composition	f_9	2300	Composition 1 (N=5)
	f_{10}	2400	Composition (N=4)
	f_{11}	2600	Composition (N=5)
	f_{12}	2700	Composition (N=6)

* f_{best}: The best solution, search boundary: [-100,100].

To guarantee the fairness of the comparison, all experiments were conducted within the MATLAB environment. The Windows 11 operating system was selected, and the PC used had 64.0G of memory and a 3.40GHz CPU. The population size was configured as 30, and the maximum number of evaluations for the 10-dimensional function was 2×10^5. The parameter settings of the comparison algorithms used are presented in Table II.

TABLE II
COMPARISON ALGORITHMS AND PARAMETERS SETTING.

Algorithm	Year	Ref.	Parameters setting
WOA	2016	[39]	a=[0,2], b=1 A=[0,2], l=[-1,1], C=2*rand
EO	2020	[40]	GP=0.5, V=1, $a1$=2, $a2$=1
CSA	2022	[41]	ρ=1.0, PP=0.1, α=4.0, β=3.0, γ=2.0
WSO	2022	[42]	R=0.1
FDBPPSO	2023	[43]	v_{max}=0.5*dx, dx=ub-lb
NRBO	2024	[44]	DF=0.6
GWO	2014	[32]	a=[0,2], A=[0,2], C=2*rand
GGWO	2022	[45]	r_1=rand, r_2=rand
FCGWO	Present	Present	r_1=rand, r_2=rand

B. Qualitative analysis

In this section, the composition function f_{12} (with the optimal value of 2700) is used to verify the performance of FCGWO. For the convenience of observation, the dimension is set to 2, the population size is set to 4, and the maximum number of iterations is set to 50. The results are evaluated by means of the average fitness value, search history and convergence curve. The experimental results are shown in Figs. 3 and 4. As can be observed from these figures, the average fitness value of GWO fluctuates frequently and with a large amplitude of change, and there is no convergence to the optimal value even until the end of the iteration. However, the average fitness value of FCGWO converges rapidly with the progress of the iteration and successfully converges to the optimal value around the 40-th iteration.

C. Comparative result analysis

We compare FCGWO with 8 advanced algorithms including GWO and its variant GGWO. The results are shown in Table III. From the table, the overall ranking of FCGWO on CEC2022 test suite is 18, and its final ranking is the first. It performs best on f_1, f_2, f_4, f_5, f_6, f_7, f_8, and f_{12}, but does not perform well on f_{10} and f_{11}. Nevertheless, it still outperforms most of the compared algorithms. However, When ranked based on the average value of all test functions, FCGWO is still the one that performs the best.

D. Algorithm complexity analysis

Algorithm complexity is a crucial indicator for evaluating the efficiency of algorithms. We adopted the method provided in Ref. [38] to conduct algorithm complexity (Complexity=$(\widehat{T_2}-T_1)/T_0$) tests on all the algorithms listed in Table II. The running results are shown in Table IV. Among them, the benchmark time T_0 for the experimental platform to execute specific programs is 0.007410200s. As can be seen from the table, the complexity of FCGWO is 186.6382769696, which is higher than that of GWO (86.6090011066). This is because in FCGWO, the FDB-based method has to calculate the FDB scores for every individual. Meanwhile, the chaos learning strategy demands information exchange among individuals. Compared with the comparison algorithms, the increased complexity of FCGWO is acceptable on the premise that its performance has been significantly improved.

TABLE III
RESULTS OF COMPARING METHODS ON CEC2022 BENCHMARK FUNCTION WITH D10.

| Fun	Index	WOA	EO	CSA	WSO	FDBPPSO	NRBO	GWO	GGWO	FCGWO
f_1	Mean	6826.97845782	308.20896238	337.53822584	4025.85155846	608.66542803	907.08888933	1199.81842648	328.23219998	300.00000000
	Std	3716.59649983	13.01589383	24.98225879	2107.89668590	1690.52039635	873.55503596	1608.68184284	8.39527152	0.00000000
	Best	1407.04625289	300.00000663	308.26343394	944.74000837	300.00025222	373.41250337	307.11620131	314.18521954	300.00000000
	Worst	14331.98459252	344.24738811	413.18779840	9510.61532050	9559.38159166	4119.64064559	7370.05525457	340.56670718	300.00000000
	Rank	9	2	4	8	5	6	7	3	1
f_2	Mean	422.26806712	411.31152574	407.22261672	465.39558891	423.76197626	459.20782246	420.55672664	408.35534604	403.17557532
	Std	29.27710616	17.18946482	3.22414338	55.15183000	51.15353962	82.97389614	21.09862370	2.68804163	3.49436172
	Best	400.06169241	400.01584955	400.40048356	410.01140251	400.00806105	412.80053109	400.37972726	402.57314651	400.01249697
	Worst	484.88855660	475.66978588	410.01818238	635.07031876	668.95672602	774.06896178	470.90599871	411.85668460	409.05475689
	Rank	6	4	2	9	7	8	5	3	1
f_3	Mean	627.53526896	600.34223154	608.27036451	626.56065724	612.32220968	620.94162494	601.15453578	604.74871997	600.59933273
	Std	11.84878342	1.27220814	6.06258642	8.57230051	6.25298520	8.84015283	1.43099219	1.18741380	0.25867905
	Best	610.42779748	600.00024964	601.99504713	609.97768287	602.60733560	608.31037938	600.01087797	603.17271828	600.14901798
	Worst	659.71470448	606.80676985	629.33486582	641.93698571	629.31325910	635.11338166	605.55140372	608.38945491	601.16782913
	Rank	9	1	5	8	6	7	3	4	2
f_4	Mean	836.12272375	812.65884810	822.77735435	838.63854673	819.51491978	828.13310627	814.81320500	818.93468140	805.80608043
	Std	15.84286281	5.46905199	9.25127911	11.71557345	7.64449810	7.88036112	5.70930056	3.60816038	1.79581810
	Best	811.94035197	803.97983624	810.27313808	823.27297455	805.68724148	811.68769636	806.58368653	809.40838252	803.28287786
	Worst	886.56143009	825.86886996	842.76575088	865.03897932	832.28503915	847.32228982	827.77643803	824.31859656	810.93415568
	Rank	8	2	6	9	5	7	3	4	1
f_5	Mean	1216.86009401	900.29795942	907.08701129	1161.30734825	1172.41532631	1001.97511010	906.95197262	903.35479462	900.05963023
	Std	213.22679152	0.46059117	13.24535260	118.79580571	193.85098809	112.78137404	12.61487891	0.86743289	0.08778122
	Best	949.65281685	900.00000191	900.53032638	966.02217370	947.20476288	903.54717466	900.03025907	902.23038055	900.00337179
	Worst	1596.44749007	901.44147790	964.93224560	1344.98635281	1662.17157284	1437.88360411	950.10647781	904.95931804	900.41567813
	Rank	9	2	5	7	8	6	4	3	1
f_6	Mean	3591.71153601	4944.34381342	5743522.71384283	4260.50192836	2816.04824854	3485.60603817	5628.61311315	12388.95508238	2043.12271762
	Std	1741.75581588	2284.46994508	4350125.72333780	2209.78966177	2171.47661250	1485.36238362	2164.44997921	7562.30540164	174.18758177
	Best	1880.39153034	2035.07323004	388029.23308304	1917.28341588	1812.91171185	1813.06372259	1913.95314387	2248.06084577	1882.70823360
	Worst	8056.14445264	8200.63279635	20170869.77421270	8124.90901674	8069.37022178	7882.39122857	8128.13467716	33893.23761558	2773.55801055
	Rank	4	6	9	5	2	3	7	8	1
f_7	Mean	2054.81820391	2022.54292194	2040.39744245	2074.31639894	2056.54515649	2056.57293545	2024.21003771	2027.35854343	2018.96017686
	Std	23.31218483	9.07935932	11.36058218	26.70130761	16.67275761	22.58369908	12.97209106	3.68867567	7.19438378
	Best	2021.31946387	2000.07300122	2018.93216598	2033.88708855	2033.76194060	2026.04495622	2000.03248020	2018.21942115	2004.24285486
	Worst	2122.23685208	2044.19595832	2072.34834035	2132.83550564	2103.24555412	2118.24103170	2056.26547797	2032.85210800	2027.76790565
	Rank	6	2	5	9	7	8	3	4	1
f_8	Mean	2229.57557733	2218.55554611	2228.44872305	2238.59144153	2233.07800236	2232.20173102	2219.62116389	2218.49233240	2217.48988951
	Std	4.75116922	6.78423736	4.66986579	24.63637482	31.15041872	21.59828524	8.51556123	6.51664624	8.03147430
	Best	2218.76602728	2201.16710156	2211.79033342	2223.77147561	2209.21169302	2215.91846930	2201.35939888	2209.43795165	2205.61245566
	Worst	2242.36099795	2224.48900886	2238.49665393	2356.44150676	2351.71667921	2344.40645805	2228.06985337	2226.42918292	2226.35712040
	Rank	6	3	5	9	8	7	4	2	1
f_9	Mean	2536.55000254	2529.28438271	2532.64949411	2623.99742535	2556.92218619	2555.75374855	2560.90110666	2530.22000963	2529.28438271
	Std	28.99042734	0.00000000	3.41398095	57.86769060	54.85307705	33.35680381	26.69497013	0.28817766	0.00000001
	Best	2529.29185089	2529.28438271	2529.75944341	2532.84130666	2529.28438271	2529.36213595	2529.28554609	2529.77319843	2529.28438271
	Worst	2676.21751975	2529.28438271	2547.29310971	2702.41267893	2712.62305556	2648.80330624	2628.33931624	2530.82955519	2529.28438279
	Rank	5	1	4	9	7	6	8	3	2
f_{10}	Mean	2576.31156730	2571.13839588	2500.63619418	2573.22937666	2569.99509290	2591.02002819	2571.88488880	2500.50897261	2561.66677150
	Std	136.86171714	68.29474517	0.16445779	72.95178021	93.88978514	60.02734097	55.82343125	0.09224148	54.57885814
	Best	2500.43261186	2500.15332793	2500.38235488	2501.03717174	2500.51322607	2500.50543578	2451.51785602	2500.28940693	2500.25591687
	Worst	3045.57231243	2747.33207487	2500.94684418	2676.46636249	2873.90467734	2643.73567578	2620.27531333	2500.75219172	2614.21376718
	Rank	8	5	2	7	4	9	6	1	3
f_{11}	Mean	2784.93157921	2690.51504040	2631.68780692	2903.26412630	2844.67998703	2867.38217597	2790.61011286	2650.90006016	2690.00796867
	Std	151.61559233	165.32750980	21.96263435	181.21153652	196.28241684	191.58058508	174.49202362	7.07533798	153.92396789
	Best	2600.21145421	2600.00001002	2620.20845013	2705.50332349	2600.08979884	2703.14479231	2600.14338004	2625.22181451	2600.00000459
	Worst	3184.13345031	3183.56567710	2745.91009487	3182.25845279	3186.22605619	3312.44771104	3183.14361459	2663.92917852	3000.00150263
	Rank	5	4	1	9	7	8	6	2	3
f_{12}	Mean	2892.42256118	2863.48621648	2864.43038441	2888.84005281	2871.25673023	2868.78211872	2868.01237672	2862.20437655	2861.40955827
	Std	41.12774199	1.15747175	1.39663135	31.11568230	9.51073369	10.86479851	8.59355309	1.20041229	1.74256609
	Best	2863.27026769	2858.78647348	2860.03864617	2864.92206525	2862.41960862	2861.80973160	2858.75865262	2859.87286609	2859.11106244
	Worst	3049.34961003	2865.46861178	2866.48079200	2985.86155377	2902.62555823	2917.54761193	2890.72748541	2864.44810457	2864.82683614
	Rank	9	3	4	8	7	6	5	2	1
Total rank		84	35	52	97	73	81	61	39	18
Final rank		8	2	4	9	6	7	5	3	1
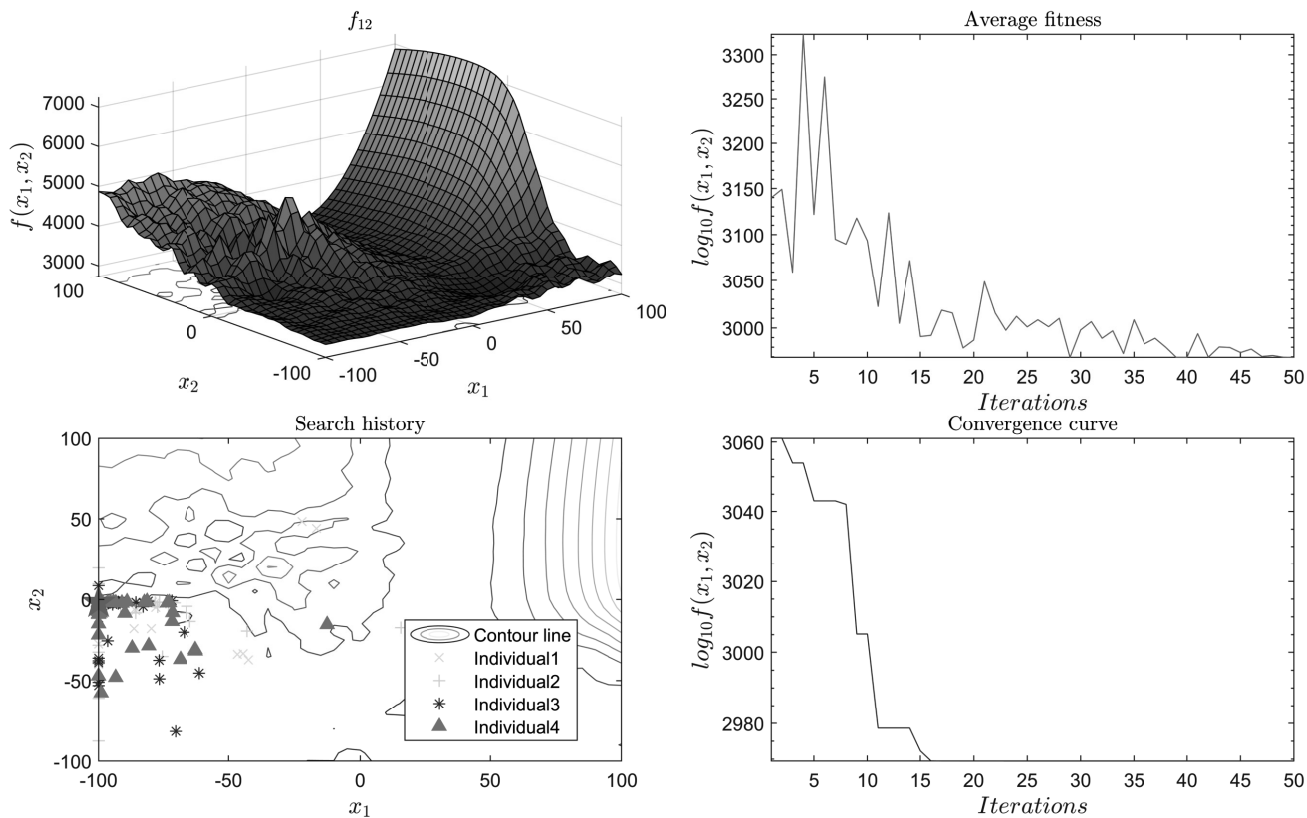
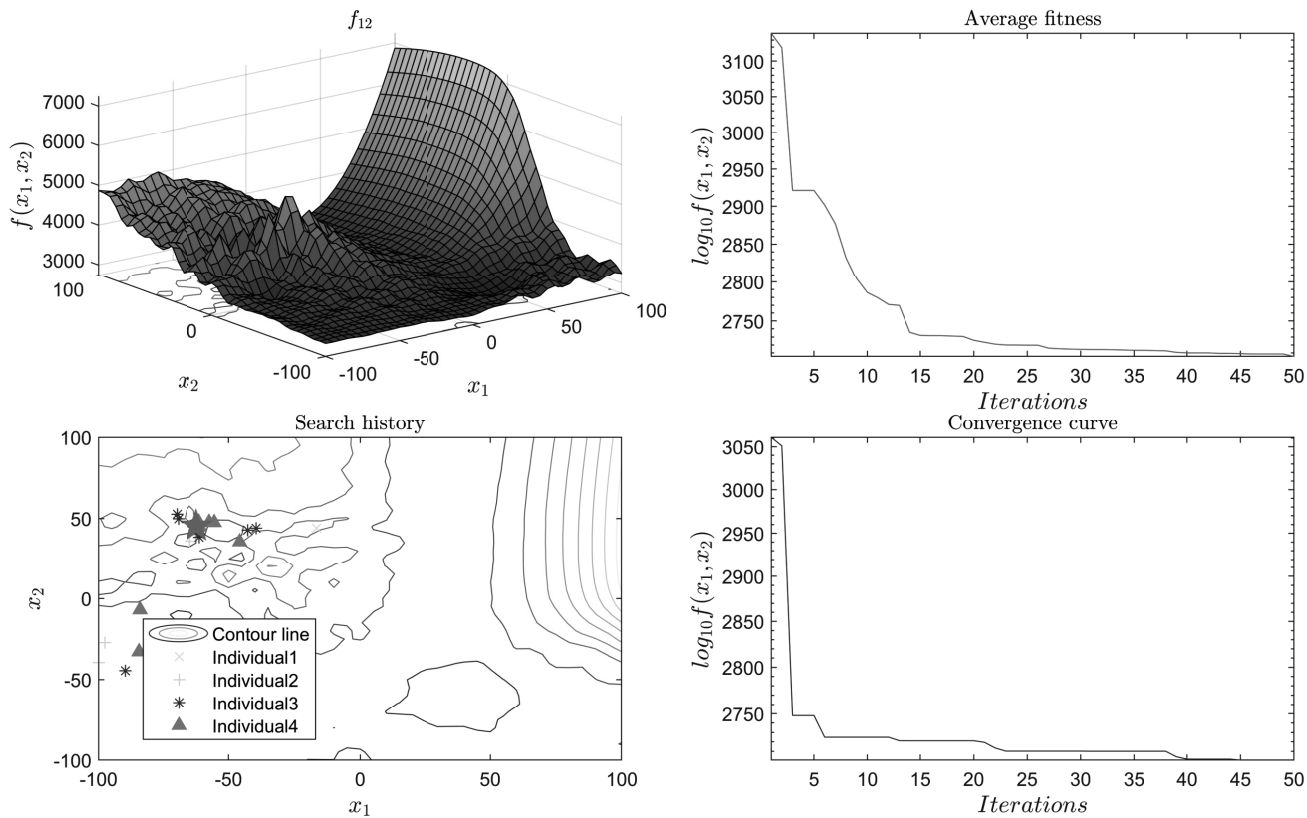Fig. 3: Search history of GWO for f_{12}.

Fig. 4: Search history of FCGWO for f_{12}.

TABLE IV
ALGORITHM COMPLEXITY RESULTS.

Algorithm	T_1 (s)	$Std.T_2$	$\widehat{T_2}$	Complexity	Rank
WOA	2.182438200	0.0623455524	2.464457660	38.0582791288	1
EO	1.989095200	0.0404146368	2.560955660	77.1720682303	3
CSA	1.972022700	0.0480198844	6.400217520	597.5810126582	9
WSO	1.967703100	0.0375867569	2.483471080	69.6024371812	2
FDBPPSO	1.997944400	0.2540771789	3.861757880	253.0750694988	6
NRBO	1.986421000	0.0780597141	4.657287280	360.4797819222	7
GWO	1.990168900	0.0378524262	2.631958920	86.6090011066	4
GGWO	1.983537400	0.0887515428	5.132916500	425.0059512564	8
FCGWO	1.986060000	0.0425510958	3.380971360	186.6382769696	5

E. Convergence performance analysis

In this part, we analyze the average convergence performance of the algorithm using the basic function f_4, and the results are presented in Fig. 5. From the figure, it's clear that the proposed FCGWO achieves the highest convergence accuracy and a favorable convergence speed for the tested functions. Compared with GWO, its convergence performance has been notably enhanced. This improvement can be credited to the FDB selection method and the chaos learning strategy that we've adopted.

F. Friedman test and Friedman alignment rank test

The Friedman test, a non-parametric statistic method, is employed to detect whether there is a significant difference in the population distribution [34]. It assesses the differences among groups by converting the original data into ranks, while Friedman alignment rank test calculates ranks based on considering the alignment relationship of the data to test for differences among groups [46]. The latter generally has higher test power and is applicable to scenarios where the data has specific structures or relationships.

Table V hows the experimental results of FCGWO and the compared algorithms. Evidently, FCGWO ranks first, with the p-value of 3.62612399E-10 and 1.56561313E-12, which are far smaller than 0.05, indicating that there are significant differences among these algorithms.

TABLE V
FRIEDMAN TEST AND FRIEDMAN ALIGNMENT RANK TEST
RESULTS.

Algorithm	Friedman test		Friedman aligned test	
	MeanRank	Rank	MeanRank	Rank
WOA	7.00000000000	8	76.00000000000	8
EO	2.91666666667	2	35.50000000000	3
CSA	4.33333333333	4	46.58333333333	4
WSO	8.08333333333	9	86.50000000000	9
FDBPPSO	6.08333333333	6	65.66666666667	6
NRBO	6.75000000000	7	66.91666666667	7
GWO	5.08333333333	5	49.33333333333	5
GGWO	3.25000000000	3	32.66666666667	2
FCGWO	1.50000000000	1	31.33333333333	1
p-value	3.62612399E-10		1.56561313E-12	

G. Wilcoxon signed rank test

In this section, the Wilcoxon signed rank test [47] is utilized to conduct pairwise tests on the differences between FCGWO and all the compared algorithms. For the convenience of observation, the final statistical results are presented in the form of average, as shown in Table IV. R- and R+ represent, respectively, the average rank sum of FCGWO's outperformance and inferiority to the comparison algorithms in solving the 12 functions. '+', '-' and '=' indicate that FCGWO outperforms, outperforms and does not significantly differ from the comparison algorithm for the 12 functions, respectively. It is clear from Table VI that for most of the test functions, FCGWO has a distinct advantage over the algorithms listed in Table II.

TABLE VI
WILCOXON TEST (AVERAGE) RESULTS.

FCGWO vs.	p-value	R+	R-	+/=/-
WOA	0.03092965031	26.66666666667	438.33333333333	11/1/0
EO	0.20313055138	143.16666666667	321.83333333333	5/6/1
CSA	0.05642746890	56.58333333333	408.41666666667	10/1/1
WSO	0.00887911882	19.16666666667	445.83333333333	11/1/0
FDBPPSO	0.07279154066	61.33333333333	403.66666666667	10/2/0
NRBO	0.00003138668	11.41666666667	453.58333333333	12/0/0
GWO	0.07408774576	65.33333333333	399.66666666667	8/4/0
GGWO	0.08618477862	80.41666666667	384.58333333333	9/2/1

V. APPLICATION RESULTS OF FCGWO TO PV MODULE
MODEL UNDER DYNAMIC WEATHER

For the time-varying weather conditions, the parameter estimation performance of FCGWO in such situations is of crucial importance. In this section, FCGWO is applied to the widely known Shell ST40 module under various climatic conditions.

A. Introduction to PV module and parameter settings

The Shell ST40 module consists of an overall structure formed by 25 copper indium diselenide (CIS)-based solar cells connected in series (N_s=1 and N_p=25). It has been widely applied to grid connection in the field of photovoltaics. The electrical characteristics at standard test conditions (STC, $1000W/m^2$ and $25°C$) are peak power P_{mpp}=40W, peak power voltage V_{mpp}=16.6V, peak power current I_{mpp}=2.41A, open circuit voltage V_{oc}=23.3V, short circuit current I_{sc}=2.68A, $series\ fuse\ rating = 5A$, and minimum peak power $P_{mpp_{min}}$=36W. Temperature coefficients at low irradiance are αP_{mpp}=-0.6%/$°C$, αV_{mpp}=-100mV%/$°C$, αI_{sc}=+0.35mA%/$°C$, and αV_{oc}=-100mV%/$°C$. And, the nominal operating cell temperature T_{NOCT} is $47°C$, for details in [48].

According to the method provided in [49], we set the search upper and lower limits as follows: $I_{ph} \in [0, 2I_{sc}(G,T)](A), I_{sd} \in [1E - 6, 50](\mu A), R_s \in [0, 2](\Omega), R_p \in [0.001, 5000](\Omega), n \in [1, 4]$. The $I_{sc}(G,T)$ under non-standard conditions of irradiance (G) and temperature (T) can be determined according to Eq.(15) through the electrical characteristics parameters under STC.

$$I_{sc}(G,T) = I_{sc-STC} * \frac{G}{G_{STC}} + \alpha I_{sc} * (T - T_{STC}) \quad (15)$$

The datasets used (see [48, 49]) are widely applied to evaluate the performance of parameter estimation methods. All the experimental parameters remain consistent with those in Section IV.
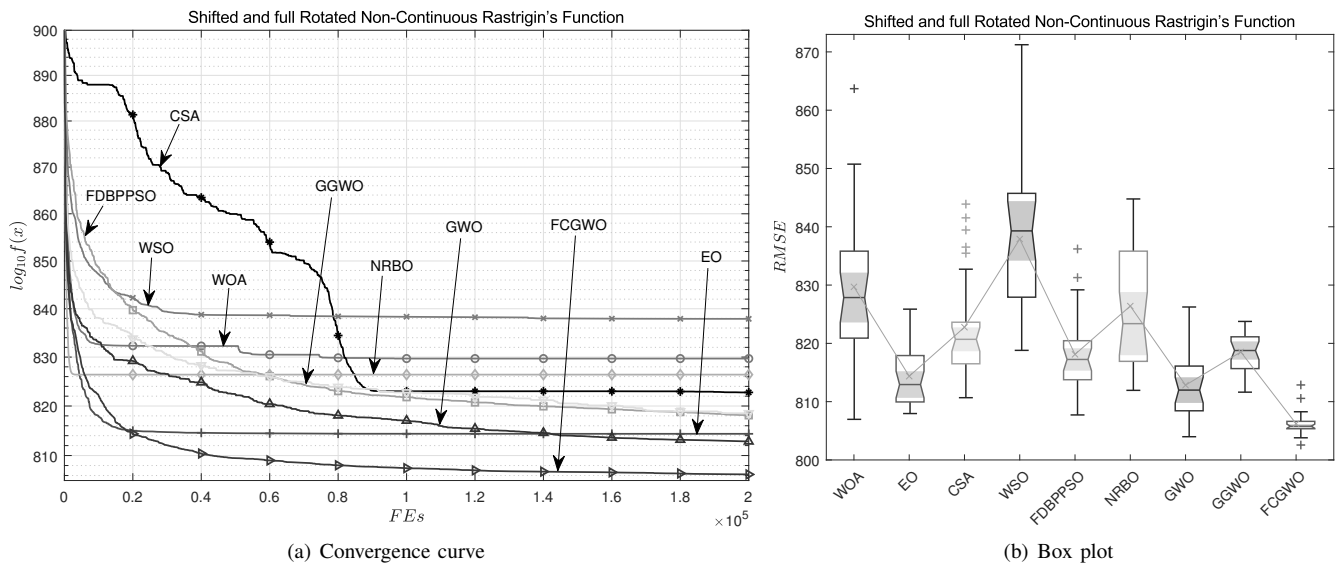
(a) Convergence curve

(b) Box plot

Fig. 5: Convergence curve and box plot on f_4 of CEC2022.

B. Standard test conditions (STC) estimated results

Standard test conditions (STC) serve as the industry benchmark for the testing and application of solar panels. Therefore, we first use FCGWO to estimate the parameters of the PV module model under STC. The results consist of the optimal RMSE, the corresponding estimated parameters, and the running time, as shown in Table VII. From this, the RMSE value of FCGWO is 0.00073409853, which is much better than that of GGWO, GWO, and other comparison algorithms. It is also the only one among the algorithms that reaches the accuracy level of 1E-04. The running time of FCGWO is 9.8154160000s, which is not outstanding. However, it is still acceptable and applicable among many algorithms.

Fig. 6 presents the convergence curve and the box plot. As can be seen from Fig. 6(a), FCGWO has the fastest convergence speed, outperforming NRBOG, GWO, and EO. It obtains the best RMSE when the number of function evaluations (FEs) is 0.2×10^5, and then it keeps converging, which reflects its capability to avoid getting stuck in local optima. The convergence speed and accuracy performance of FDBPPSO, WOA, and WSO are all not satisfactory. These algorithms get trapped in local optimal solutions at an early stage and are unable to break free successfully in the later stages. The '+' in Fig. 6(b) represents outliers, and the broken line is the average value of RMSE. It is clear that the box plot of FCGWO is the flattest, demonstrating the best stability. Its average value is also the most excellent. On the other hand, Fig. 7 illustrates the population diversity of FCGWO and GWO under the current conditions. From the figure, throughout the entire iteration stage, FCGWO demonstrates a far superior population diversity compared to GWO. This is attributed to the FDB-based method, which takes into account the distances among the population. By doing so, it facilitates the expansion of the population's search range, thus augmenting the diversity. The above analysis has confirmed that FCGWO has a satisfactory accuracy for the PV module model under STC.

C. Different irradiances estimated results

Under STC, FCGWO exhibits a highly competitive estimation accuracy. However, parameter estimation under time-varying weather conditions is of more practical application value. In this section, FCGWOG estimates the parameters of the ST40 PV module under $25°C$ and different irradiance levels ($1000W/m^2$, $800W/m^2$, $600W/m^2$, $400W/m^2$). For the sake of simplicity, Table VIII shows the performance indicators under different irradiance levels at $25°C$. It is evident that the accuracy of FCGWO is guaranteed under various irradiance conditions. The optimal RMSE values obtained are 0.00073409853, 0.00077412459, 0.00067403574, and 0.00063072457 respectively, which are far superior to those of the comparison algorithms. The accuracy does not fluctuate with the change of irradiance, demonstrating extremely strong stability.

In addition, once the model parameters have been estimated, it is straightforward to obtain the output current and power corresponding to the voltage. This enables the reconstruction of the I-V and P-V characteristic curves, as shown in Fig. 8. Both relative error (RE) curve of the current and individual absolute error (IAE) curve of the power indicate that the error between the estimated results of FCGWO and the measured values is very small, being controlled within the range of 0.035. The fitting curves also show that the estimated data by FCGWO closely aligns with the measured data across the entire voltage range. In conclusion, regardless of the irradiance conditions, FCGWO is far superior to the algorithms based on the RMSE evaluation criterion and has excellent parameter estimation accuracy for the ST40 PV module model. The above phenomena profoundly prove that FCGWO is a promising algorithm, demonstrating its strength in being applied to actual PV modules.

D. Different temperatures estimated results

It can be known from Eq.(15) that temperature also has an impact on the estimated parameters of the PV module. In this work, the climatic conditions of temperature are regarded as another estimation scenario. Specifically, FCGWO is used

TABLE VII
PARAMETER ESTIMATION RESULTS OF ST40 PV MODULE ON STC.

| Parameter	WOA	EO	CSA	WSO	FDBPPSO	NRBO	GWO	GGWO	FCGWO
I_{ph} (A)	2.64916211877	2.65535728937	2.65900301983	2.65611806859	2.66303708466	2.65234716596	2.65611783143	2.65432773667	2.67579981477
I_{sd1} (A)	1.07268222E-05	3.92963990E-05	4.22999114E-05	1.42540926E-05	1.46840904E-06	1.88786807E-05	4.42364272E-06	2.02874607E-05	1.00000000E-12
I_{sd2} (A)	7.59756307E-06	5.45740109E-06	1.97698435E-05	3.36722769E-05	1.44843700E-05	4.67128820E-05	6.35348230E-06	9.32194896E-07	1.00000000E-12
I_{sd3} (A)	1.89443312E-06	1.29192791E-05	7.05121387E-06	1.34815272E-05	3.52630482E-06	1.90863839E-07	1.06687475E-12	8.72144794E-06	1.52880247E-06
R_s (Ω)	0.02644340518	0.02238643410	0.02294811822	0.02193324374	0.02496720702	0.02727262843	0.02417523124	0.02309026956	0.02650538101
R_p (Ω)	1067.921843224	4992.376779371	68.924811741	1168.187725494	18.906240406	4950.462545783	54.955882069	3456.359412132	8.514249251
n_1	2.56561667303	3.85836952671	2.71522070597	2.73464935499	2.70897115642	3.99585849140	3.61763846289	3.46846827453	4.00000000000
n_2	2.71085730056	3.96511119554	3.07204619092	3.63428805510	3.40280615148	2.30548864818	1.66266543930	1.92374628246	4.00000000000
n_3	1.52466319938	1.75765677030	1.68153059962	1.76522994331	1.59183122682	1.32721673103	1.21458698356	1.70676871931	1.50027992927
RMSE	0.00836434733	0.00862210455	0.00790469779	0.00918331626	0.00516514832	0.00612795997	0.00644777266	0.00801695734	0.00073409853
Run time (s)	7.9271082000	8.3184712000	12.3881064000	8.1844898000	8.8515613000	8.8194779000	8.0886438000	9.9766095000	9.8154160000

(a) Convergence curve
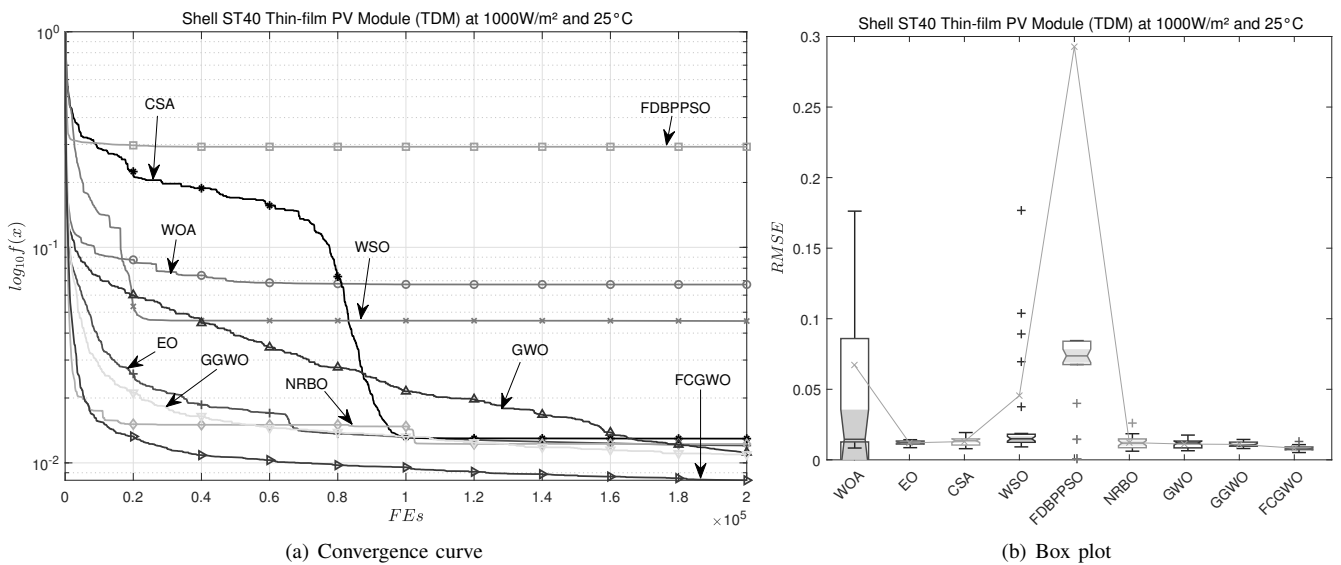
(b) Box plot

Fig. 6: Convergence curve and box plot of ST40 PV module on STC.
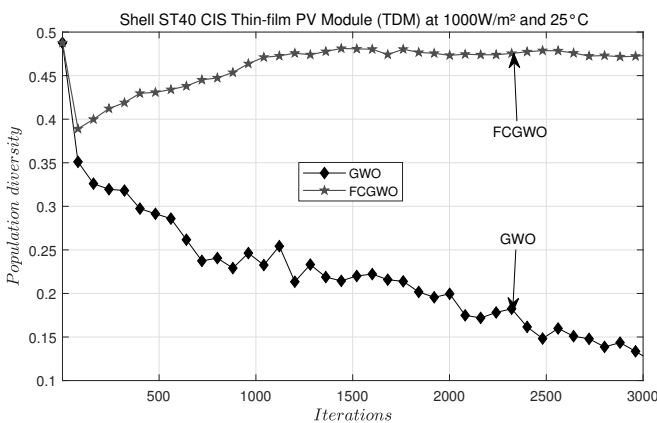

Fig. 7: Population diversity of FCGWO and GWO of ST40 PV module on STC.

to estimate the parameters of the ST40 module under the irradiance of $1000W/m^2$ and different temperatures ($25°C$, $40°C$, $50°C$, $60°C$). Among them, $25°C$ is used as a benchmark for comparison. The experimental results in a concise representation are shown in Table IX. When compared to irradiance, the impact of temperature exerts a more significant influence on the estimation accuracy. Under the conditions of $40°C$ and $50°C$, FCGWO achieved the minimum RMSE values of 0.00132493187 and 0.00176046248 respectively, outperforming GGWO, GWO and other comparison algorithms. CSA obtained RMSE values of 0.00211079943 and 0.00214253010, ranking second. The advantage of FCGWO is not as obvious as that under irradiance conditions. As for $60°C$, the estimation accuracy of all algorithms has declined significantly. Among them, the optimal RMSE of FCGWO is 0.02175865777, which is inferior to that of FDBPPSO, CSA, NRBO and EO, but the relative difference is not large.

Fig. 9 presents the fitting and error curves at different temperatures estimated by FCGWO. The maximum power points corresponding to different temperatures have changed significantly. The error at $60°C$ fluctuates the most at the maximum power point, while it is stable at $25°C$, $40°C$ and $50°C$. Nevertheless, the fitting curves also show strong consistency. Overall, FCGWO achieves the best accuracy performance at different temperatures, outperforming the comparison algorithms and being capable of handling this model.

TABLE VIII
ESTIMATED RESULTS OF COMPARING METHODS FOR ST40 PV MODULE AT $25°C$ AND DIFFERENT IRRADIANCES.

Irradiance	Index	WOA	EO	CSA	WSO	FDBPPSO	NRBO	GWO	GGWO	FCGWO
$1000W/m^2$	Mean	0.06721116631	0.01204112964	0.01295811884	0.04551338051	0.29276872876	0.01224290699	0.01117882494	0.01094843029	0.00830618634
	Std	0.11701955178	0.00153139702	0.00292229704	0.10378767348	0.71588283775	0.00438979043	0.00285441739	0.00188185008	0.00162687299
	Best	0.00836434733	0.00862210455	0.00790469779	0.00918331626	0.00516514832	0.00612795997	0.00644777266	0.00801695734	0.00073409853
	Worst	0.39320253374	0.01427674110	0.01933590311	0.56002802758	2.40341558249	0.02605560989	0.01754852792	0.01444569637	0.01301165023
	Rank	7	8	5	9	2	3	4	6	1
$800W/m^2$	Mean	0.01963370106	0.01216584317	0.01197362137	0.02036520265	0.23550058825	0.01081611713	0.01189017551	0.01065548658	0.00854379738
	Std	0.01656674351	0.00451340799	0.00207957039	0.02141534633	0.49660381988	0.00210506397	0.01052820472	0.00116984430	0.00151244374
	Best	0.00829928513	0.00622577076	0.00661980883	0.00822084955	0.00492782339	0.00737144726	0.00762045298	0.00844480695	0.00077412459
	Worst	0.07155568219	0.03410054755	0.01589793669	0.09386802570	1.91546643735	0.01383944856	0.06695073904	0.01304025527	0.01232912957
	Rank	8	3	4	7	2	5	6	9	1
$600W/m^2$	Mean	0.01184651075	0.00825852977	0.00721669733	0.01952735045	0.14587282918	0.00804223933	0.00957909400	0.00783581643	0.00597688904
	Std	0.00591318803	0.00146194609	0.00135397811	0.05100795002	0.36907668748	0.00099000139	0.00362531151	0.00027552551	0.00148204514
	Best	0.00743650658	0.00614977254	0.00366491486	0.00675697138	0.00290225167	0.00679076709	0.00666773176	0.00739075627	0.00067403574
	Worst	0.02621211056	0.01204895136	0.00902127893	0.28698096217	1.45958850455	0.01076378484	0.02049263784	0.00842204241	0.00782938079
	Rank	9	4	3	6	2	7	5	8	1
$400W/m^2$	Mean	0.01676956608	0.00703928161	0.00607007735	0.00867852535	0.02193244658	0.00779598450	0.00805077012	0.00703783862	0.00533379426
	Std	0.03032737648	0.00081788088	0.00098192026	0.00450437402	0.05068704636	0.00175912907	0.00171437992	0.00044250166	0.00122443802
	Best	0.00693688897	0.00486269581	0.00407929670	0.00461120001	0.00179250989	0.00436135007	0.00656048095	0.00532654856	0.00063072457
	Worst	0.17164122651	0.00815888191	0.00779174241	0.03103014110	0.17172332512	0.01381595239	0.01298981175	0.00741466401	0.00682560261
	Total rank	33	21	15	27	8	19	23	30	4
	Final rank	9	5	3	7	2	4	6	8	1

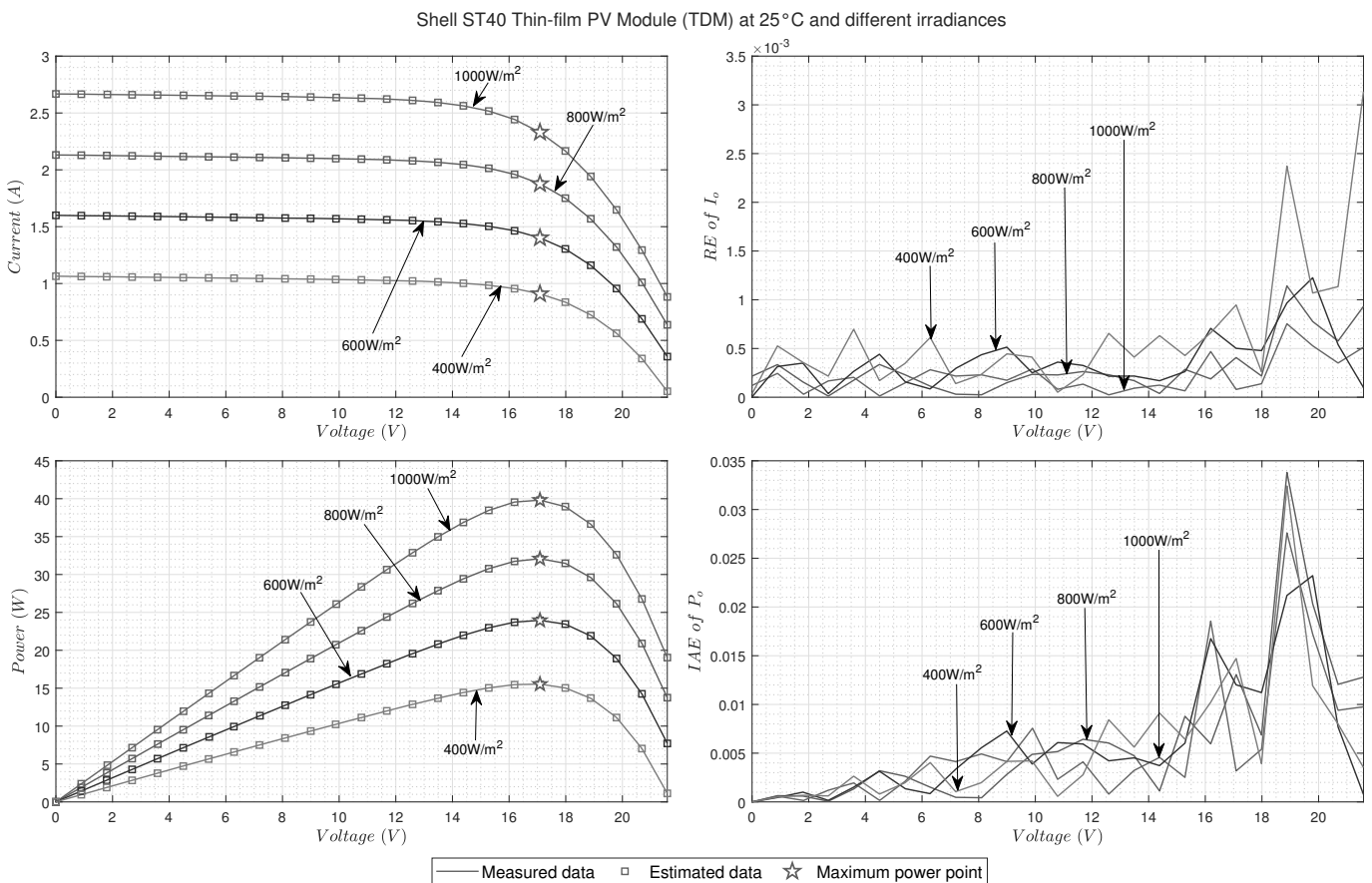Shell ST40 Thin-film PV Module (TDM) at 25°C and different irradiances

Fig. 8: Different irradiances results for ST40 PV module estimated by FCGWO.

TABLE IX
ESTIMATED RESULTS OF COMPARING METHODS FOR ST40 PV MODULE AT $1000W/m^2$ DIFFERENT TEMPERATURES.

| Temperature	Index	WOA	EO	CSA	WSO	FDBPPSO	NRBO	GWO	GGWO	FCGWO
25°C	Mean	0.06721116631	0.01204112964	0.01295811884	0.04551338051	0.29276872876	0.01224290699	0.01117882494	0.01094843029	0.00830618634
	Std	0.11701955178	0.00153139702	0.00292229704	0.10378767348	0.71588283775	0.00438979043	0.00285441739	0.00188185008	0.00162687299
	Best	0.00836434733	0.00862210455	0.00790469779	0.00918331626	0.00516514832	0.00612795997	0.00644777266	0.00801695734	0.00073409853
	Worst	0.39320253374	0.01427674110	0.01933590311	0.56002802758	2.40341558249	0.02605560989	0.01754852792	0.01444569637	0.01301165023
	Rank	7	8	5	9	2	3	4	6	1
40°C	Mean	0.03540048689	0.00988174960	0.00882551230	0.04376503112	0.22851702282	0.00914435247	0.00813456888	0.00921255730	0.00669327277
	Std	0.08587193776	0.00161692941	0.00296457705	0.10845174613	0.45930691632	0.00211189851	0.00210808243	0.00149045695	0.00082007841
	Best	0.00263768415	0.00685442997	0.00211079943	0.00605919207	0.00433773252	0.00438995937	0.00539297035	0.00644012811	0.00132493187
	Worst	0.43862408421	0.01382439217	0.01307850363	0.43704480334	2.35696767081	0.01274597877	0.01363098161	0.01281586353	0.00809006729
	Rank	3	9	2	7	4	5	6	8	1
50°C	Mean	0.02114651282	0.006671889935	0.004450473050	0.01684146512	0.29918713847	0.009977035095	0.00702096586	0.008810710900	0.00594115358
	Std	0.04144990320	0.00361461342	0.00212135019	0.02245445679	0.60751327096	0.00588048605	0.00149707816	0.00110916303	0.00098478767
	Best	0.00603869612	0.00310559116	0.00214253010	0.00609941566	0.00227769181	0.00483293184	0.00599700051	0.00659888728	0.00176046248
	Worst	0.17963636662	0.02540283091	0.01173850151	0.11628926385	2.35523136299	0.02623711723	0.01290074450	0.01056332746	0.00763558607
	Rank	7	4	2	8	3	5	6	9	1
60°C	Mean	0.02478987898	0.02265201966	0.02330790290	0.13501752446	0.16658183981	0.02571934286	0.02417104691	0.02365981317	0.02247960978
	Std	0.00446907511	0.00096474566	0.00348940924	0.22543516814	0.20930534843	0.00587001964	0.00210833538	0.00097039941	0.00052488117
	Best	0.02225513821	0.02144622860	0.02124445170	0.02224913984	0.02095655972	0.02135961818	0.02229973688	0.02246145982	0.02175865777
	Worst	0.03968531320	0.02605400736	0.03446511264	0.89582175120	1.03305902883	0.04906451912	0.02989768413	0.02682526128	0.02434815957
	Rank	7	4	2	6	1	3	8	9	5
Total rank		24	25	11	30	10	16	24	32	8
Total rank		5.5	7	3	8	2	4	5.5	9	1
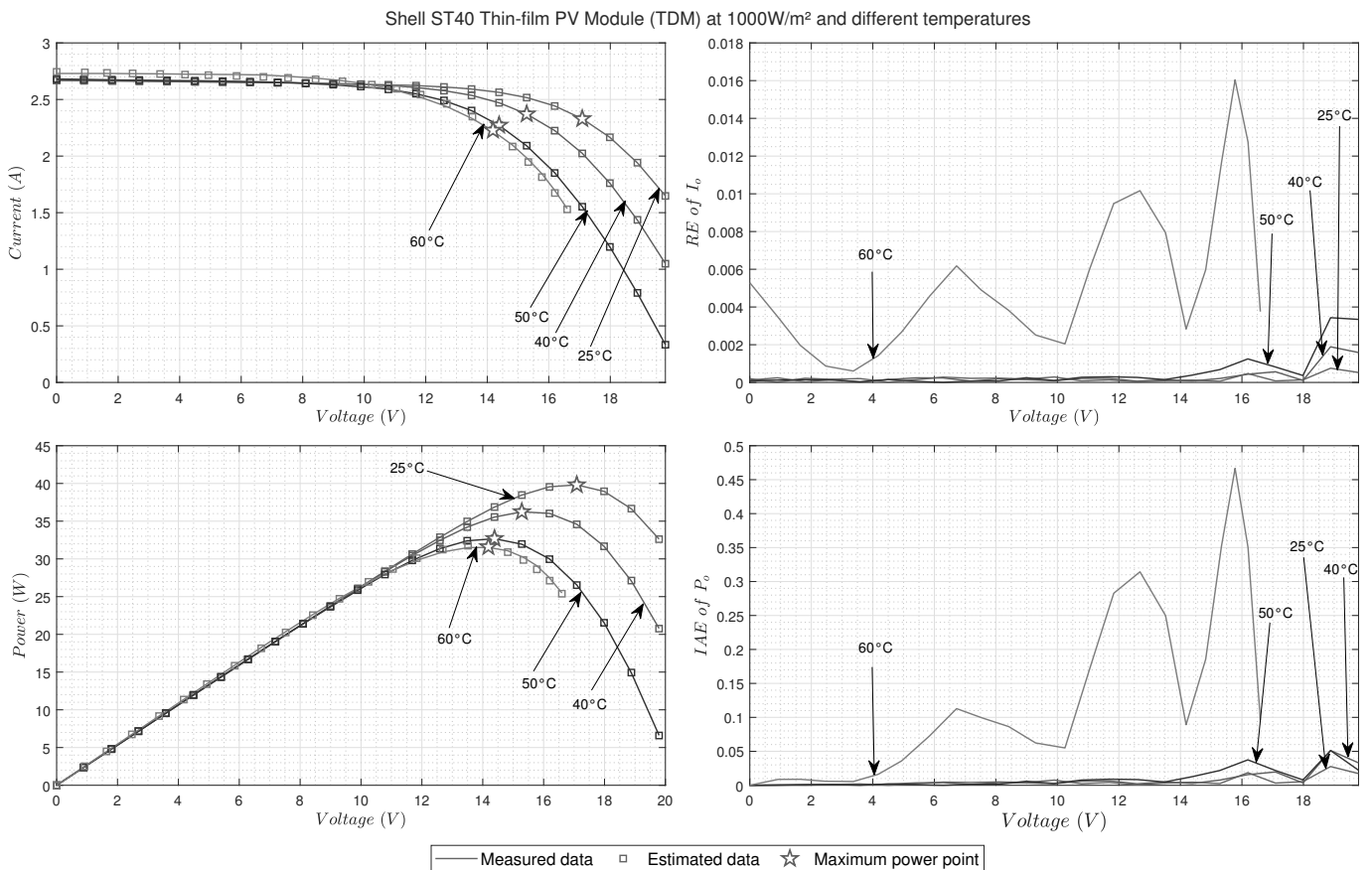
Fig. 9: Different temperatures results for ST40 PV module estimated by FCGWO.

E. Results analysis and discussion

As mentioned previously, the performance of the algorithms for estimating the parameters of PV module under dynamic weather conditions has been demonstrated from different perspectives. As is evident from Eq.(1), the objective of the model parameters exhibits the characteristics of nonlinearity, implicitness, and multimodality, which requires the algorithms to have powerful searching capabilities and is extremely challenging. The ultimate aim of this problem is to achieve the highest possible estimation accuracy, and based on the best ranking as shown in Fig. 10, the smaller the area enclosed by the radar chart's chain, the better the overall performance of the algorithm. Combining the results of Subsections V-B and V-C, it can be observed that the change of weather undoubtedly affects the accuracy of the estimated parameters. Nevertheless, FCGWO has achieved the optimal overall solution and demonstrated the best performance. In summary, FCGWO outperforms both GGWO and GWO significantly. This further validates the practicality and effectiveness of the improvements proposed in this paper for estimating PV modules. FCGWO's performance surpasses that of the compared algorithms, and it holds great promise as a valuable tool for estimating PV models.
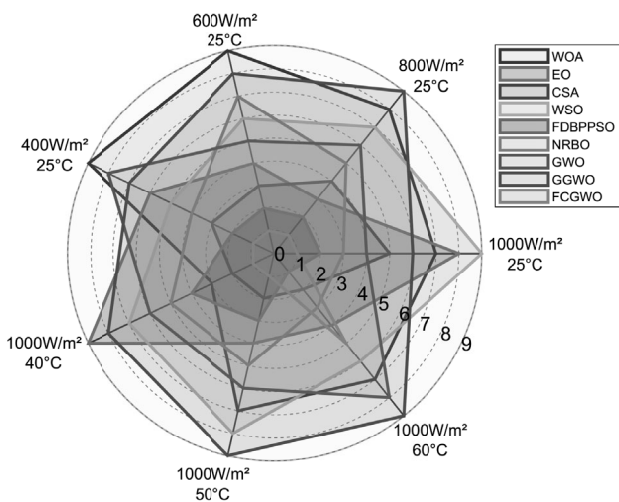

Fig. 10: Radar map of PV model estimation ranking under dynamic weather conditions.

VI. CONCLUSION

Aiming at the problem of estimating the parameters of triple diode PV modules under dynamic weather conditions, this paper proposes an enhanced grey wolf optimization algorithm (FCGWO). The algorithm incorporates the FDB selection method into the chaos learning strategy to improve the convergence performance and population diversity of GWO. Firstly, chaos learning expands the search range of GWO based on the ergodic and random characteristics in the improved Tent chaotic map, enabling the algorithm to explore more potential search areas. Secondly, by utilizing the guiding effect in chaos learning, the average position of the population gradually approaches the optimal solution, thereby enhancing the global exploitation performance. Thirdly, the FDB selection method factors in the impact of fitness and distance of solutions. This allows it to strike

a balance between the algorithm's global exploration and local exploitation capabilities, and boosts the likelihood of the algorithm breaking free from local optima. FCGWO is evaluated against 8 comparison algorithms on CEC2022 test suite. The Friedman and Friedman aligned rank, as well as Wilcoxon signed rank test, confirm that FCGWO is significantly superior to the comparison algorithms. Finally, FCGWO is applied to the actual PV module (Shell ST40) model for TDM modeling. The results under different irradiance and temperature conditions indicate that this method has the best parameter estimation accuracy, exhibits performance exceeding that of the comparison algorithms, and has a strong potential to become a valuable tool for estimating PV models.

However, the running efficiency of FCGWO is not outstanding, and it is only utilized for addressing the parameter estimation problem under single-objective independent tasks. In future work, we will continuously optimize the efficiency of this method, expand the multi-objective and multi-task versions, and study new forms of PV modeling and objective functions. In addition, expanding its application to more PV problems, such as PV array configuration, heliostat field optimization, and maximum power point tracking, will also be the research directions.

REFERENCES

[1] B. M. Opeyemi, "Path to sustainable energy consumption: The possibility of substituting renewable energy for non-renewable energy," *Energy*, vol. 228, p. 120519, 2021.

[2] K. He, Y. Zhang, Y. Wang, and R. Zhou, "Solving power system economic emission dispatch problem under complex constraints via dimension differential learn butterfly optimization algorithm with FDC-based," *Computers & Industrial Engineering*, vol. 197, p. 110568, 2024.

[3] T. Qiu, L. Wang, Y. Lu, M. Zhang, W. Qin, S. Wang, and L. Wang, "Potential assessment of photovoltaic power generation in China," *Renewable and Sustainable Energy Reviews*, vol. 154, p. 111900, 2022.

[4] M. A. E. Sattar, A. Al Sumaiti, H. Ali, and A. A. Z. Diab, "Marine predators algorithm for parameters estimation of photovoltaic modules considering various weather conditions," *Neural Computing and Applications*, vol. 33, no. 18, pp. 11 799–11 819, 2021.

[5] Y. Chaibi, A. Allouhi, M. Malvoni, M. Salhi, and R. Saadani, "Solar irradiance and temperature influence on the photovoltaic cell equivalent-circuit models," *Solar Energy*, vol. 188, pp. 1102–1110, 2019.

[6] D. S. H. Chan and J. C. H. Phang, "Analytical methods for the extraction of solar-cell single- and double-diode model parameters from I-V characteristics," *IEEE Transactions on Electron Devices*, vol. 34, no. 2, pp. 286–293, 1987.

[7] A. Younis, A. Bakhit, M. Onsa, and M. Hashim, "A comprehensive and critical review of bio-inspired metaheuristic frameworks for extracting parameters of solar cell single and double diode models," *Energy Reports*, vol. 8, pp. 7085–7106, 2022.

[8] H. Saleem and S. Karmalkar, "An analytical method to extract the physical parameters of a solar cell from four points on the illuminated $J-V$ curve," *IEEE Electron Device Letters*, vol. 30, no. 4, pp. 349–352, 2009.

[9] N. Aoun and N. Bailek, "Evaluation of mathematical methods to characterize the electrical parameters of photovoltaic modules," *Energy Conversion and Management*, vol. 193, pp. 25–38, 2019.

[10] R. Zhou, Y. Zhang, X. Sun, H. Liu, and Y. Cai, "MSWOA: Multi-

strategy whale optimization algorithm for engineering applications," *Engineering Letters*, vol. 32, no. 8, pp. 1603–1615, 2024.

[11] Q. Zhang and X. Guo, "Dual-population firefly algorithm based on gender differences for detecting protein complexes," *Engineering Letters*, vol. 32, no. 5, pp. 1062–1072, 2024.

[12] J. Qian, Y. Peng, H. Zheng, and X. Wang, "Application of improved seagull optimization algorithm on optimal allocation optimizations of distributed generation," *Engineering Letters*, vol. 31, no. 3, pp. 1151–1159, 2023.

[13] J. Wang, R. Sun, Y. Zheng, R. Song, and Y. Li, "White shark optimizer based time-optimal trajectory planning for supernumerary robotic limbs," *Engineering Letters*, vol. 32, no. 7, pp. 1448–1464, 2024.

[14] Y. Hou, C. Wang, W. Dong, and L. Dang, "An improved particle swarm optimization algorithm for the distribution of fresh products," *Engineering Letters*, vol. 31, no. 2, pp. 494–503, 2023.

[15] M. Qais, H. M. Hasanien, S. Alghuwainem, and A. S. Nouh, "Coyote optimization algorithm for parameters extraction of three-diode photovoltaic models of photovoltaic modules," *Energy*, vol. 187, p. 116001, 2019.

[16] M. H. Qais, H. M. Hasanien, and S. Alghuwainem, "Parameters extraction of three-diode photovoltaic model using computation and Harris hawks optimization," *Energy*, vol. 195, no. 15, pp. 117 040.1–117 040.13, 2020.

[17] D. Wang, X. Sun, H. Kang, Y. Shen, and Q. Chen, "Heterogeneous differential evolution algorithm for parameter estimation of solar photovoltaic models," *Energy Reports*, vol. 8, pp. 4724–4746, 2022.

[18] M. A. Soliman, A. Al-Durra, and H. M. Hasanien, "Electrical parameters identification of three-diode photovoltaic model based on equilibrium optimizer algorithm," *IEEE Access*, vol. 9, pp. 41 891–41 901, 2021.

[19] M. A. Soliman, H. M. Hasanien, and A. Alkuhayli, "Marine predators algorithm for parameters identification of triple-diode photovoltaic models," *IEEE Access*, vol. 8, pp. 155 832–155 842, 2020.

[20] K. Yu, J. Liang, B. Qu, X. Chen, and H. Wang, "Parameters identification of photovoltaic models using an improved JAYA optimization algorithm," *Energy Conversion and Management*, vol. 150, pp. 742–753, 10 2017.

[21] M. Abdel-Basset, R. Mohamed, A. El-Fergany, M. Abouhawwash, and S. S. Askar, "Parameters identification of PV triple-diode model using improved generalized normal distribution algorithm," *Mathematics*, vol. 9, no. 9, pp. 1–23, 2021.

[22] M. Abd Elaziz and D. Oliva, "Parameter estimation of solar cells diode models by an improved opposition-based whale optimization algorithm," *Energy Conversion and Management*, vol. 171, pp. 1843–1859, 2018.

[23] S. Li, "Parameter extraction of photovoltaic models using an improved teaching-learning-based optimization," *Energy Conversion and Management*, vol. 186, pp. 293–305, 2019.

[24] M. Abdel-Basset, R. Mohamed, and S. Mirjalili, "A novel whale optimization algorithm integrated with nelder–mead simplex for multi-objective optimization problems," *Knowledge-Based Systems*, vol. 212, pp. 106 619–106 645, 2021.

[25] W. Long, T. Wu, M. Xu, T. Mingzhu, and S. Cai, "Parameters identification of photovoltaic models by using an enhanced adaptive butterfly optimization algorithm," *Energy*, vol. 103, pp. 120 750–120 766, 2021.

[26] Y. Sharma and L. C. Saikia, "Automatic generation control of a multi-area ST – Thermal power system using grey wolf optimizer algorithm based classical controllers," *International Journal of Electrical Power & Energy Systems*, vol. 73, pp. 853–862, 2015.

[27] T. Jayabarathi, T. Raghunathan, B. Adarsh, and P. N. Suganthan, "Economic dispatch using hybrid grey wolf optimizer," *Energy*, vol. 111, pp. 630–641, 2016.

[28] S. Gupta and K. Deep, "A novel random walk grey wolf optimizer," *Swarm and Evolutionary Computation*, vol. 44, pp. 101–112, 2019.

[29] S. Jiao, G. Chong, C. Huang, H. Hu, M. Wang, A. A. Heidari, H. Chen, and X. Zhao, "Orthogonally adapted Harris hawks optimization for parameter estimation of photovoltaic models," *Energy*, vol. 203, p. 117804, 2020.

[30] X. Gao, Y. Cui, J. Hu, G. Xu, Z. Wang, J. H. Qu, and H. Wang, "Parameter extraction of solar cell models using improved shuffled complex evolution algorithm," *Energy Conversion and Management*, vol. 157, pp. 460–479, 2018.

[31] M. Mostafa, H. Rezk, M. Aly, and E. M. Ahmed, "A new strategy based on slime mould algorithm to extract the optimal model parameters of solar PV panel," *Sustainable Energy Technologies and Assessments*, vol. 42, p. 100849, 2020.

[32] S. Mirjalili, S. M. Mirjalili, and A. Lewis, "Grey wolf optimizer," *Advances in Engineering Software*, vol. 69, no. 3, p. 46–61, 2014.

[33] H. T. Kahraman, S. Aras, and E. Gedikli, "Fitness-distance balance (FDB): A new selection method for meta-heuristic search algorithms," *Knowledge-Based Systems*, vol. 190, p. 105169, 2020.

[34] K. He, Y. Zhang, Y.-K. Wang, R.-H. Zhou, and H.-Z. Zhang, "EABOA: Enhanced adaptive butterfly optimization algorithm for numerical optimization and engineering design problems," *Alexandria Engineering Journal*, vol. 87, pp. 543–573, 2024.

[35] M.-H. Nadimi-Shahraki, S. Taghian, and S. M. Mirjalili, "An improved grey wolf optimizer for solving engineering problems," *Expert Systems With Applications*, vol. 166, p. 113917, 2021.

[36] X. Ru, "Parameter extraction of photovoltaic model based on butterfly optimization algorithm with chaos learning strategy," *Solar Energy*, vol. 269, p. 112353, 2024.

[37] L. Yao, P. Yuan, C.-Y. Tsai, T. Zhang, Y. Lu, and S. Ding, "ESO: An enhanced snake optimizer for real-world engineering problems," *Expert Systems with Applications*, vol. 230, p. 120594, 2023.

[38] A. Kumar, K. V. Price, A. W. Mohamed, and A. A. Hadi, "Problem definitions and evaluation criteria for the CEC 2022 special session and competition on single objective bound constrained numerical optimization," IEEE Congress on Evolutionary Computation (CEC), Nanyang Technological University, Singapore, Tech. Rep., 2021.

[39] Mirjalili, Seyedali, Lewis, and Andrew, "The whale optimization algorithm," *Advances in engineering software*, vol. 95, pp. 51–67, 2016.

[40] A. Faramarzi, M. Heidarinejad, B. Stephens, and S. Mirjalili, "Equilibrium optimizer: A novel optimization algorithm," *Knowledge-Based Systems*, vol. 191, pp. 105 190–105 230, 2020.

[41] M. S. Braik, "Chameleon swarm algorithm: A bio-inspired optimizer for solving engineering design problems," *Expert Systems With Applications*, vol. 174, no. C, pp. 114 685–114 709, 2021.

[42] T. S. L. V. Ayyarao, N. S. S. Ramakrishna, R. M. Elavarasan, N. Polumahanthi, M. Rambabu, G. Saini, B. Khan, and B. Alatas, "War strategy optimization algorithm: A new effective metaheuristic algorithm for global optimization," *IEEE Access*, vol. 10, pp. 25 073–25 105, 2022.

[43] S. Duman, H. T. Kahraman, B. Korkmaz, H. Bakır, U. Guvenc, and C. Yilmaz, *Improved Phasor Particle Swarm Optimization with Fitness Distance Balance for Optimal Power Flow Problem of Hybrid AC/DC Power Grids*. Cham: Springer International Publishing, 01 2023, pp. 307–336.

[44] R. Sowmya, P. Manoharan, and P. Jangir, "Newton-raphson-based optimizer: A new population-based metaheuristic algorithm for con-

tinuous optimization problems," *Engineering Applications of Artificial Intelligence*, vol. 128, p. 107532, 2024.

[45] M.-H. Nadimi-Shahraki, S. Taghian, S. Mirjalili, H. Zamani, and A. Bahreininejad, "GGWO: Gaze cues learning-based grey wolf optimizer and its applications for solving engineering problems," *Journal of Computational Science*, vol. 61, p. 101636, 2022.

[46] J. Derrac, S. García, D. Molina, and F. Herrera, "A practical tutorial on the use of nonparametric statistical tests as a methodology for comparing evolutionary and swarm intelligence algorithms," *Swarm and Evolutionary Computation*, vol. 1, pp. 3–18, 2011.

[47] D. W. Zimmerman and B. D. Zumbo, "Relative power of the wilcoxon test, the friedman test, and repeated-measures anova on ranks," *Journal of Experimental Education*, vol. 62, no. 1, pp. 75–86, 1993.

[48] J. Shi, Y. Chen, A. A. Heidari, Z. Cai, H. Chen, Y. Chen, and G. Liang, "Environment random interaction of rime optimization with nelder-mead simplex for parameter estimation of photovoltaic models," *Scientific Reports*, vol. 14, no. 1, p. 15701, 2024.

[49] I. Choulli, M. Elyaqouti, E. hanafi Arjdal, D. Ben hmamou, D. Saadaoui, S. Lidaighbi, A. Elhammoudy, I. Abazine, and Y. El aidi idrissi, "DIWJAYA: JAYA driven by individual weights for enhanced photovoltaic model parameter estimation," *Energy Conversion and Management*, vol. 305, p. 118258, 2024.